Conformation of sLe^x Tetrasaccharide, Free in Solution and Bound to E-, P-, and L-Selectin[†,‡]

Leszek Poppe,* Gregory S. Brown, John S. Philo, Pandurang V. Nikrad, and Bhavana H. Shah

Contribution from Amgen Inc., 3200 Walnut Street, Boulder, Colorado 80301

Received April 1, 1996[⊗]

Abstract: The conformations of the NeuAcα2(I)→3Galβ1(II)→4[Fucα1(III)→3]GlcNAc-O-CH$_3$ tetrasaccharide (sLe^x), in aqueous solution and bound to E-, P-, and L-selectin have been determined using high resolution NMR spectroscopy. In the free ligand, the conformation of glycosidic linkage I is disordered with $\{\Phi_I, \Psi_I\}$ sampling values close to $\{-60°, 0°\}$, $\{-100°, -50°\}$, and $\{180°, 0°\}$. The trisaccharide portion is rigid and characterized by $\{\Phi_{II}, \Psi_{II}; \Phi_{III}, \Psi_{III}\} = \{46°, 18°; 48°, 24°\}$. The measured dissociation rates and equilibrium binding constants, $\{k_{off}, K_D\}$, were $\{164 \pm 24\ s^{-1}, 0.72 \pm 0.4\ mM\}$, $\{522 \pm 166\ s^{-1}, 7.8 \pm 1.0\ mM\}$, and $\{1080 \pm 167\ s^{-1}, 3.9 \pm 0.6\ mM\}$ at 300 K for E-, P-, and L-selectin, respectively. The bound conformations of the ligand were calculated from the full relaxation matrix analysis of transferred-NOE spectra for E- and P-selectin or by using a two-spin approximation for the L-selectin complex. Both E- and P-selectin recognize the $\{-60°, 0°\}$ conformation of sLe^x while the $\{-100°, -50°\}$ conformer is probably recognized by L-selectin. The conformation of the branched trisaccharide portion in the bound state remains close to the conformation of the free ligand. In the E-, P-, and L-selectin complexes the GalH4 proton is in the vicinity of protein aromatic protons, most likely Tyr94 and/or Tyr48.

Introduction

Sialyl Lewis^x tetrasaccharide, NeuAcα2→3Galβ1→4[Fucα1→3]GlcNac (sLe^x), is involved in the adhesion of leukocytes and neutrophils to vascular endothelial cells during normal and pathogenic inflammatory responses. Three structurally similar transmembrane glycoproteins, E- , P- , and L-selectin, recognize the sLe^x epitope through a calcium-dependent lectin domain.[1] The way in which selectins recognize carbohydrate is of fundamental importance for generating small molecule antagonists and has been intensively explored in the past few years.[2] The current models for the three-dimensional structure of sLe^x/E- and P-selectin complexes are based on the X-ray structure of unliganded E-selectin,[3] the force-field derived model of sLe^x,[4] and a substantial amount of data on affinity changes upon either genetic modification of E-[3,5] and P-[6] selectins or chemical modification of the sLe^x ligand.[7] Recently, three independent transferred-NOE studies have appeared, shedding more light on sLe^x conformation when bound to E-selectin.[8] Despite the different results between ref 8c and refs 8a,b regarding the NeuAcα2→3Gal linkage conformation, all approaches were qualitative in nature, leaving the definition of bound-state conformation still open.

Here we describe the conformation of sLe^x, both in the free and bound states, as determined by quantitative analysis of NMR

* The address for correspondence: Dr. Leszek Poppe, Amgen Inc., 3200 Walnut St., AB-1A, Boulder, CO 80301. Telephone: 303-541-1677, E-mail: lpoppe@amgen.com, FAX: 303-938-6217.

[†] **Keywords**: sLe^x, carbohydrate conformation, transferred-NOE, E-selectin, P-selectin, L-selectin.

[‡] **Abbreviations**: sLe^x, sialyl Lewis X; NOE, nuclear Overhauser effect; CRD, carbohydrate recognition domain; EGF, epidermal growth factor.

[⊗] Abstract published in *Advance ACS Abstracts,* February 1, 1997.

(1) For recent review see (a) Lasky, L. A. *Annu. Rev. Biochem.* **1995**, *64*, 113−139. (b) Bertozzi, C. R. *Chem. Biol.* **1995**, *2*, 703−708. (c) Rosen, S. D.; Bertozzi, C. R. *Curr. Op. Cell Biol.* **1994**, *6*, 663−673. (d) Bevilacqua, M. P. *Annu. Rev. Immunol.* **1993**, *11*, 767−804.

(2) See, for example: (a) Dasgupta, F.; Rao, B. N. N. *Exp. Opin. Invest. Drugs* **1994**, *3*, 709−724. (b) Kogan, T. P.; Dupre, B.; Keller, K. M.; Scott, I. L.; Bui, H.; Market, R. V.; Beck, P. J.; Voytus, J. A.; Revelle, B. M.; Scott, D. *J. Med. Chem.* **1995**, *38*, 4976−4984. (c) Toepfer, A.; Kretzschmar, G.; Bartnik, E. *Tetrahedron Lett.* **1995**, *36*, 9161−9164. (d) Kogan, T. P.; Dupré, B.; Keller, K. M.; Scott, I. L.; Bui, H.; Market, R. V.; Beck, P. J.; Voytus, J. A.; Revelle, B. M.; Scott, D. *J. Med. Chem.* **1996**, *38*, 4976−4984.

(3) Graves, B. J.; Crowther, R. L.; Chandran, Ch.; Rumberger, J. M.; Li, S.; Huang, K.-S.; Presky, D. H.; Familletti, P. C.; Wolitzky, B. A.; Burns, D. K. *Nature* **1994**, *367*, 532−538.

(4) (a) Ichikawa, Y.; Lin, Y. C.; Dumas, D. P.; Shen, G.-J.; Garcia-Junceda, E.; Williams, M. A.; Bayer, R.; Ketcham, C.; Walker, L. E.; Paulson, J. C.; Wong, C. H. *J. Am. Chem. Soc.* **1992**, *114*, 9283−9298. (b) Lin, Y. C.; Hummel, C. W.; Huang, D. H.; Ichikawa, Y.; Nicolaou, K. C.; Wong, C. H. *J. Am. Chem. Soc.* **1992**, *114*, 5452−5454. (c) Ball, G. E.; O'Neill, R. A.; Schultz, J. E.; Lowe, J. B.; Weston, B. W.; Nagy, J. O.; Brown, E. G.; Hobbs, G. J.; Bednarsky, M. D. *J. Am. Chem. Soc.* **1992**, *114*, 5449−5451. (d) Rao, B. N. N.; Anderson, M. B.; Musser, J. H.; Gilbert, J. H.; Schaefer, M. E.; Foxall, C.; Brandley, B. K. *J. Biol. Chem.* **1994**, *269*, 19663−19666.

(5) (a) Erbe, D. V.; Wolitzky, B. A.; Presta, L. G.; Norton, Ch. R.; Ramos, R. J.; Burns, D. K.; Rumberger, J. M.; Rao, B. N. N.; Foxall, C.; Brandley, B. K.; Lasky, L. A. *J. Cell Biol.* **1992**, *119*, 215−227. (b) Kogan, T. P.; Revelle, B. M.; Tapp, S.; Scott, D.; Beck, P. J. *J. Biol. Chem.* **1994**, *270*, 14047−14055.

(6) (a) Erbe, D. V.; Watson, S. R.; Presta, L. G.; Wolitzky, B. A.; Foxall, C.; Brandley, B. K.; Lasky, L. A. *J. Cell Biol*. **1993**, *120*, 1227−1235. (b) Hollenbaugh, D.; Bajorath, J.; Stenkamp, R.; Aruffo, A. *Biochemistry* **1993**, *32*, 2960−2966. (c) Bajorath, J.; Hollenbaugh, D.; King, G.; Harte, J.; Eustice, D. C.; Darveau, R. P.; Aruffo, A. *Biochemistry* **1994**, *33*, 1332−1339. (d) Revelle, B. M.; Scott, D.; Kogan, T. P.; Zheng, J.; Beck, P. J. *J. Biol. Chem.* **1996**, *271*, 4289−4297.

(7) (a) Huang, H.; Wong, C. H. *J. Org. Chem.* **1995**, *60*, 3100−3106. (b) Uchiyama, T.; Vassilev, V. P.; Kajimoto, T.; Wong, W.; Huang, H.; Lin, C. C.; Wong C. H. *J. Am. Chem. Soc.* **1995**, *117*, 5395−5396. (c) Ramphal, J. Y.; Zheng, Z. L.; Perez, C.; Walker, L. E.; DeFrees, S. A.; Gaeta, F. C. A. *J. Med. Chem.* **1994**, *37*, 3459−3463. (d) Nelson, R. M.; Dolich, S.; Aruffo, A.; Cecconi, O.; Bevilacqua, M. P. *J. Clin. Invest.* **1993**, *91*, 1157−1166. (e) Musser, J. H.; Rao, N.; Nashed, M.; Dasgupta, F.; Abbas, S.; Nematalla, A.; Date, V.; Foxall, C.; Asa, D.; James, P.; Tyrrell, D.; Brandley, B. K. In *Trends in Receptor Research*; Claassen, V., Ed.; 1993; pp 33−40. (f) Manning, D. D.; Bertozzi, C. R.; Pohl, N. L.; Rosen, S. D.; Kiessling, L. L. *J. Org. Chem.* **1995**, *60*, 6254−6255. (g) Thoma, G.; Schwarzenbach, F.; Duthaler, R. O. *J. Org. Chem.* **1996**, *61*, 514−524. (h) Stahl, W.; Sprengard, U.; Kretzschmar, G.; Kunz, H. *Angew. Chem., Int. Ed. Engl.* **1994**, *33*, 2096−2098. (i) Thoma, G.; Schwarzenbach, F.; Duthaler, R. O. *J. Org. Chem.* **1996**, *61*, 514−524. (j) Ramphal, J. Y.; Hiroshige, M.; Lou, B.; Gaudino, J.; Hayashi, M.; Chen, S. M.; Chiang, L. C.; Gaeta, F. C. A.; DeFrees, S. A. *J. Med. Chem.* **1996**, *39*, 1357−1360. (k) Bamford, M. J.; Bird, M.; Gore, P. M.; Holmes, D. S.; Priest, R.; Prodger, J. C.; Saez, V. *Bioorg. Med. Chem. Lett.* **1996**, *6*, 239−244. (l) Sprengard, U.; Kunz, H.; Hüls, Ch.; Schmidt, W.; Seiffge, D.; Kretzschmar, U. *Bioorg. Med. Chem. Lett.* **1996**, *6*, 509−514.

S0002-7863(96)01070-0 CCC: $14.00 © 1997 American Chemical Society

data. This differs from previous work in which the NMR constraints were mostly used to support force-field based molecular modeling.[4ab,9ab] In the present study the three-dimensional model of the free ligand is calculated from interglycosidic coupling constants and distance constraints. The latter are obtained from NOE measurements involving hydroxyl protons in conditions of slow chemical exchange.[10]

The dissociation rates and equilibrium binding constants for the sLe^x /E-, P-, and L-selectin complexes are obtained from the temperature and composition dependent selective relaxation rates of the ligand proton.

The bound conformations of sLe^x with E- and P- selectins are calculated from the full relaxation matrix analysis of the 2D transferred-NOE spectra. Based on hydrodynamic studies we use the prolate ellipsoid model for the motion of sLe^x/selectin complexes in solution. This allows better definition of the bound conformation and determination of the ligand orientation relative to the major axis. The conformation of sLe^x bound to L-selectin was calculated from the interproton distances obtained by first-order analysis of the 2D tranferred-NOE spectrum.

Finally, contacts between sLe^x and the three selectins were probed by protein to ligand magnetization transfer experiments.

Methods

Determination of the Ligand Conformation. The conformation of the carbohydrate, defined in terms of glycosidic torsional angles $\{\Phi,\Psi\}$, can be derived from the NMR constraints by minimization of the following expression:

$$T = \sum_{ij,kl} (d_{ij}^{\mathrm{calc}} - d_{ij}^{\mathrm{exp}})^2 + \sum_{kl} (J_{kl}^{\mathrm{calc}} - J_{kl}^{\mathrm{exp}})^2 \qquad (1)$$

where d_{ij}^{calc} and d_{ij}^{exp} are the calculated and experimental interproton distances and J_{kl}^{calc} and J_{kl}^{exp} are calculated and experimental values for the interglycosidic $^{13}C-^{1}H$ coupling constants, respectively. The geometry of the pyranose rings, interglycosidic C−O−C bond angles, as well as pendant group torsions were frozen during the optimization of the dihedral angles Φ and Ψ. The starting geometry, G0, of sLe^x was built from the X-ray coordinates of the monosaccharide units and refined by energy minimization using cff91 force field included in the BIOSYM software. The d_{ij}^{calc} were calculated from Cartesian coordinates transformed upon $\{\Phi,\Psi\}$ rotations. The uncertainty of the experimental values was included in the form of the following equation:

$$d_{ij}^{\mathrm{exp}} = d_{ij}^{\mathrm{m}} + \Delta_{ij} \times \sin \gamma_{ij} \qquad (2)$$

where d_{ij}^{m} is the median value and Δ_{ij} is the error bound derived from the NOE experiment (Tables 2 and 5). In order to keep d_{ij}^{exp} within $\pm\Delta_{ij}$ interval during the optimizations the dummy factor $\sin \gamma_{ij}$ was introduced which was independently optimized for each constraint. The J_{kl}^{exp} were expressed in an analogous way. The J_{kl}^{calc} were calculated from the Karplus equation parametrized for carbohydrates[11]

$$^3J = 5.7 \cos^2 \Theta - 0.6 \cos \Theta + 0.5 \qquad (3)$$

where Θ is either Φ or Ψ.

Alternatively conformation of the free and bound ligands can be determined from the full relaxation matrix analysis of the 2D NOESY and 2D transferred-NOESY spectra, respectively. In this case structural parameters were obtained by minimizing the expression

$$T = \sum_{\tau_m} \sum_{ij} (I_{ij}^{\mathrm{calc}}(\tau_m) - I_{ij}^{\mathrm{exp}}(\tau_m))^2 \qquad (4)$$

where the first and the second summation runs over different mixing times and different cross-peaks, respectively. The $I_{ij}^{\mathrm{calc}}(\tau_m)$ and $I_{ij}^{\mathrm{exp}}(\tau_m)$ denote calculated and experimental cross-peak intensities at mixing time τ_m, respectively. The $I_{ij}^{\mathrm{calc}}(\tau_m)$ were calculated using matrix algebra closely following the procedures described by Ni[13] and London et al.[14] The matrices $\mathbf{R}_f$, $\mathbf{R}_b$, $\mathbf{K}$, and $\mathbf{I}_o$ were constructed as described below.

Since the spectra were recorded at the conditions where the interproton cross-relaxation rates in the free ligand are close to zero, the relaxation matrix $\mathbf{R}_f$, was diagonal with experimentally determined longitudinal relaxation times, T_{1i}^{-1}.

The relaxation matrix for the bound ligand was calculated from the formulas[15]

$$R_{ij}^{\mathrm{b}} = -\frac{C}{r_{ij}^6}\left(\frac{(3\cos^2\Theta - 1)^2}{24D_\perp} + \frac{3\cos^2\Theta \sin^2\Theta}{D_\parallel + 5D_\perp} + \frac{3}{4}\frac{\sin^4\Theta}{4D_\parallel + 2D_\perp}\right) \qquad (5)$$

$$R_{ij}^{\mathrm{b}} = -\sum_{j \neq i} R_{ij}^{\mathrm{b}}$$

where $C = 56.9 \times 10^9$ Å^6 s^{-2}, $D_\perp$ and $D_\parallel$ are rotational diffusion coefficients for the prolate ellipsoid, and Θ is the angle between the long axis and the interproton vector r_{ij}. This angle can be expressed by the trigonometrical relation:

$$\cos\Theta = \frac{z\cos\theta + y\sin\theta\sin\phi + x\sin\theta\cos\phi}{\sqrt{x^2 + y^2 + z^2}} \qquad (6)$$

where θ and ϕ are polar angles describing the orientation of the major diffusion axis in the molecular frame. During each step of the target function optimization, T, the Cartesian coordinates, x, y, and z of the ligand were generated by transforming initial coordinates upon the $\{\Phi, \Psi\}$ rotations. For the interaction between the methyl group and nonmethyl proton we used a simplified approach where the magnetization from methyl protons is localized in the center of mass of the methyl protons.[16]

(8) (a) Scheffler, K.; Ernst, B.; Katopodis, A.; Magnani, J. L.; Wang, W. T.; Weisemann, R.; Peters, T. *Angew. Chem., Int. Ed. Engl.* **1995**, *34*, 1841−1844. (b) Cooke, R. M.; Hale, R. S.; Lister, S. G.; Shah, G.; Weir, M. P. *Biochemistry* **1994**, *33*, 10591−10596. (c) Hansley, P.; McDevitt, P. J.; Brooks, I.; Trill, J. J.; Feild, J. A.; McNulty, D. E.; Connor, J. R.; Griswold, D. E.; Kumar, N. V.; Kopple, K. D.; Carr, S. A.; Dalton, B. J.; Johanson, K. *J. Biol. Chem.* **1994**, *269*, 23949−23958.

(9) (a) Rutheford, T. J.; Spackman, D. G.; Simpson, P. J.; Homans, S. W. *Glycobiology* **1994**, *4*, 59−68. (b) Mukhopadhyay, C.; Miller, K. E.; Bush, C. A. *Biopolymers* **1994**, *34*, 21−29. (c) Wormald, M. R.; Edge, C. *J. Carbohydr. Res.* **1993**, *246*, 337−344.

(10) Poppe, L.; van Halbeek, H. *Nature Struct. Biol.* **1994**, *1*, 215−216.

(11) Tvaroška, I.; Hricovini, M.; Petráková, E. *Carbohydr. Res.* **1989**, *189*, 359−362.

(12) (a) Ni, F. *Prog. NMR Spectrosc.* **1994**, *26*, 517−606. (b) Clore, G. M.; Gronenborn, A. M. *J. Magn. Reson.* **1982**, *48*, 402−417. (c) Bevilacqua, V. L.; Thomson, D. S.; Prestegard, J. H. *Biochemistry* **1990**, *29*, 5529−5537. (d) Glaudemans, C. P. J.; Lerner, L.; Daves, G. D.; Kovác, P.; Venable R.; Bax, A. *Biochemistry* **1990**, *29*, 10906−10911.

(13) Ni, F. *J. Magn. Reson.* **1992**, *96*, 651−656.

(14) London, R. E.; Perlman, M. E.; Davis, D. G. *J. Magn. Reson.* **1992**, *97*, 79−98.

(15) Woessner, D. E. *J. Chem. Phys.* **1962**, *37*, 647−659.

(16) Liu, H.; Thomas, P. D.; James, T. L. *J. Magn. Reson.* **1992**, *98*, 163−175.

The individual intensities, I_j^o, were corrected for the incomplete relaxation between the scans and nonuniform signal loss during the short spin-lock pulse (vide infra). Since both experimental and calculated intensity matrices were nonsymmetric, instead of I_{ij} in (4), the averages, $0.5(I_{ij} + I_{ji})$, have been used in the optimization.

Expression 4 was minimized by varying the global proton intensity parameter, six glycosidic and two polar angles, θ and ϕ, in eq 6. The computations were based on 24 different NOE interactions measured at five mixing times, 50, 100, 150, 200, and 300 ms, for the E-selectin complex and three mixing times, 200, 300, and 400 ms, for the P-selectin complex. To ensure that all solutions with the minimum T value in eq 4 were found, we performed systematic grid searches in the eight-dimensional parameter space using 30° steps for θ and ϕ and 15° steps for each dihedral angle. The side chains were fixed in the same rotameric states as in the free ligand (see Discussion). In order to assess the scatter of possible solutions the optimizations were restarted from over 300 randomly generated starting conditions. When evaluating the results we considered only the solutions which converged to the T values not exceeding the global minimum by more than 25%.[17] Conformations with low T values but displaying obvious steric conflicts were also rejected.

Hydrodynamic Studies. Sedimentation velocity experiments were carried out at 50 000 rpm and 293 K in a Beckman Optima XL-A analytical ultracentrifuge. E-selectin was loaded at 0.6 mg/mL in Dulbecco's PBS with calcium and magnesium. The sedimentation coefficient, s, and diffusion coefficient, D, were evaluated using the program SVEDBERG.[18] A molecular weight of 77 100 (95% confidence interval 73 900 to 79 700) was then calculated from the ratio s/D, using a partial specific volume of 0.692 g/mL determined from a self-consistent method. Calculation of the axial ratio for a prolate ellipsoid model followed the procedures of Laue et al.[19] and Ushiyama et al.[20]

Hydrodynamic measurements of E- and P-[20]selectins have shown that the shape of both proteins may be approximated by prolate ellipsoids with axial ratios of 12:1 and 19:1, respectively. Using these values the rotational diffusion constants, $D_\perp$, $D_\parallel$, calculated from the Perrin model,[21] were found to be 3.26×10^5 s^{-1}, 8.01×10^6 s^{-1} and 1.50×10^5 s^{-1}, 8.55×10^6 s^{-1} for E-selectin and P-selectin, respectively. These values were also used for the computations of relaxation matrixes in the bound state.

Determination of the Dissociation Rates and Equilibrium Binding Constants. For the quantitative analysis of transferred-NOE spectra, both the dissociation rates and the bound fraction of the ligand must be known. Only in a few studies[12c,d,22] of protein−carbohydrate interactions were these parameters estimated from the NMR data. Here we utilize the approach which is based on the relaxation measurements of an isolated proton spin from the ligand.[23] Thermodynamic and kinetic parameters for the binding of sLe^x to E-, P-, and L-selectin were based on the temperature and composition dependence of the NH3eq proton relaxation rate. Chemical shift of this proton resonance is particularly suitable for selective spin manipulations (vide infra). Also, strong dipolar interaction between geminal protons causes very fast relaxation in the bound state, favorably enhancing sensitivity of the observed relaxation rates toward temperature and composition variability.

For the binding of sLe^x to selectins, the kinetic scheme of the two-site exchange between bound (b) and free (f) forms of the ligand (L)

$$\mathrm{L_f} \underset{k_{off}}{\overset{k'_{on}}{\rightleftharpoons}} \mathrm{L_b}$$

where k_{off} is the off-rate and k'_{on} is the pseudo-first-order on-rate, $k'_{on} = k_{on}[P]$, k_{on} being the reaction on-rate and [P] the equilibrium free protein concentration. Thus the dynamics of an isolated spin, in the absence of free precession, can be described by the following equation[12a]

$$\frac{\mathrm{d}}{\mathrm{d}t}\begin{bmatrix} m_f \\ m_b \end{bmatrix} = \begin{bmatrix} R^f + k'_{on} & -k_{off} \\ -k'_{on} & R^b + k_{off} \end{bmatrix}\begin{bmatrix} m_f \\ m_b \end{bmatrix} \tag{7}$$

where R^f and R^b are the relaxation rates of the magnetization in the free (m_f) and bound (m_b) states, respectively. The R^f values were determined experimentally, whereas R^b was approximated by the following relationship[24]

$$R^b = \frac{C}{T}\exp\left(\frac{E_a}{RT}\right) \tag{8}$$

where C depends on physical constants and molecular structure which should remain the same for all temperatures and concentrations.

Temperature dependences of the off- and on-rates were expressed by using Eyring equation.[25]

The K_D's and k_{off}'s for the binding of sLe^x to the E-, P-, and L-selectins were obtained by either fitting the experimental decay rates to the values given by the first eigenvalue of the exchange matrix in eq 8[26] or by fitting signal intensities to the numerical solution of eq 7. Both C and E_a in eq 8 and the global scaling factor (for integral signal intensities) were optimized. E_a was bounded to values of 16−20 kJ/mol.[24]

Sample Preparations. The sLe^x O-methyl glycoside was purchased fom Toronto Research Chemicals Inc. The Gal-2-O-Acetyl derivative is a byproduct obtained in the synthesis of **1** (Chart 1)−(R = $-(CH_2)_8OCOOCH_3$) obtained as described previously.[27] Recombinant, soluble E-selectin was produced according to the procedure of Lobb et al.[28] The recombinant, soluble P-selectin was purified as decribed elswhere.[20] Recombinant fusion proteins, E-selectin-Ig, P-slectin-Ig, and L-selectin-Ig, were constructed, expressed, and purified as previously described.[7d] They contain signal sequence, a lectin domain, and an EGF repeat along with six (E-selectin-Ig), two

(17) This change gives statistically significant decrease of the reduced χ-square probability. For this estimation the uncertainties were obtained by dividing the optimized T value (eq 4) at global minimum by the number of fitted intensities.

(18) Philo, J. S. In *Modern Analytical Ultracentrifugation*; Schuster, T. M., Laue, T. M., Eds.; Birkhauser: Boston, 1994; pp 156−170.

(19) Laue, T. M.; Shah, B. D.; Ridgeway, T. M.; Pelletier, S. M. In *Analytical Ultracentrifugation in Biochemistry and Polymer Science*; Harding, S. E., Rowe, A. J., Eds.; Royal Society of Chemistry: Cambridge, 1992; pp 90−125.

(20) Ushiyama, S.; Laue, T. M.; Moore, K. L.; Erickson, H. P.; McEver, R. P. *J. Biol. Chem.* **1993**, *268*, 15229−15237.

(21) Cantor, C. R.; Schimmel. P. R. *Biophysical Chemistry*; Freeman, W. H. and Company: San Francisco, 1980.

(22) Kronis, K. A.; Carver, J. P. *Biochemistry* **1985**, *24*, 834−840.

(23) Valensin, G.; Kushnir, T.; Navon, G. *J. Magn. Reson.* **1982**, *46*, 23−28.

(24) Lane, A. N.; Lefèvre, J. F.; Jardetzky, O. *J. Magn. Reson.* **1986**, *66*, 201−218.

(25) Jencks, W. P. *Catalysis in Chemistry and Enzymology*; Dover Publications: New York, 1987.

(26) Bain, A. D.; Duns, G. J. *J. Magn. Reson.* **1995**, *112*, 258−260.

(27) Ratcliffe, R. M.; Venot, A. P.; Abbas, S. Z. U.S. Pat. Appl. 5,296,-594, March 22, 1994.

(28) Lobb, R. R.; Chi-Russo, G.; Leone, D. R.; Rosa, D. R.; Bixler, S.; Newman, B. M.; Luhowskyj, S.; Benjamin, Ch. D.; Douglas, I. G.; Goelz, S. E.; Hession, C.; Chow, E. P. *J. Immun.* **1991**, *147*, 124−129.

Chart 1

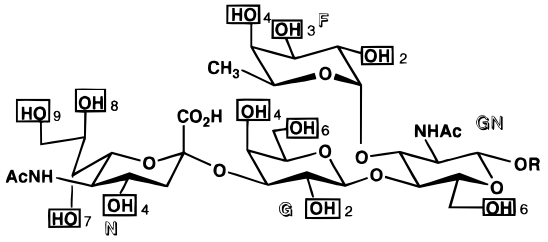

1

(P-selectin-Ig), or one (L-selectin-Ig) complement regulatory modules. The apparant molecular weight of these three fusion proteins were 250, 220, and 200 kDa, respectively. The proteins were dialized against PBS buffer containing 2 mM calcium chloride at pH = 7.4. Samples were prepared by mixing aqueous solutions of the protein and carbohydrate in desired proportions. The samples were then exchanged with deuterium oxide by three freeze−dry cycles and finally dissolved in 250 μL of D_2O. For the quantitative transferred-NOE studies the [ligand]:[protein] ratio was 20:1 for E- and P-selectin and 15:1 for L-selectin.

NMR Experiments. The NMR experiments were performed using a Bruker DRX-500 spectrometer equipped with a Nalorac 3 mm inverse broadband probe and a Bruker DRX-400 spectrometer equipped with a 5 mm inverse broadband probe. For experiments which required supercooling of the water, capillary tubes (1.2 mm o.d.) were used.

All data in H_2O/D_2O (9:1) were obtained with the standard pulse sequences where all hard 90° pulses were replaced with soft(90°_{-x})hard(90°_x) for nonexcitation of the water signal.[29] The soft pulse was 4−5 ms Gaussian shaped pulse applied at the frequency of the water signal.

The heteronuclear coupling constants were obtained from the HSQC experiment with a short (2 ms) spin-lock pulse.[30] The delay for the evolution of $^3J_{CH}$ was set to 100 ms. This delay allowed for the refocussing of the homonuclear couplings which are close to 10 Hz. The coupling constants were measured directly from the separation of the antiphase signal maxima. Alternatively, the long range cross-peaks, $^3J_{C1H3}$, may be easily reconstructed by superimposing two parts of the $^1J_{C1H1}$ cross-peak occurring in the same spectrum. The coupling constant is then determined by the best fit between the target and the trial multiplets.[31] The $^3J_{NC1-GH3}$ coupling was measured by the selective version of the same experiment.[32] The digital resolution in the transformed spectra was 0.35 Hz/pt.

The 2D transferred-NOESY experiments were recorded with the standard pulse sequence. Acquisition times were 0.35 and 0.2 s in t_2 and t_1 domains, respectively. Relaxation delays were 1.7, 2.1, and 3.1 s in spectra recorded for E-, P-, and L-selectin, respectively. For better quantitation of transferred-NOE spectra a 15 ms spin-lock pulse was applied prior to t_1 delay, in order to eliminate protein background signals.[33] The raw data were apodized by the cosine-square or Gauss-Lorentz window functions. Transformed spectra were baseline corrected and integrated using UXNMR software.

1D NOESY[34] and combined 1D DAISY[35]-NOESY experiments were obtained with a selective Gaussian or DANTE,[36] 90_x-$180_{x,y,-x,-y}$, proton excitation followed by up to two coherent magnetization tranfer steps using DANTE pulse trains.

The longitudinal relaxation rates were monitored by the selective 1D NOESY pulse sequence. Selective excitation, applied to the N3eq proton, was achieved either by a 20 ms E-BURP pulse or by a composite 90_x-$180_{x,y,-x,-y}$ DANTE pulse train of the same duration. In order to simplify spin-dynamics[37] the cross-relaxation effects were suppressed by the simultaneous irradiation at NH3ax and NH4 frequencies during the mixing times (30−250 ms) with the field strength of 60 Hz.

Selective relaxation in the rotating frame, $R_{1\rho}$, was monitored by on resonance spin-locking NH3eq magnetization with a weak, 100 Hz, B1 field. In this case all cross-relaxation pathways were blocked[37] except for cross-correlated cross-relaxation, which, for the durations the of the spin-lock times (<200 ms), may be safely ignored. The offset effects[38] on $R_{1\rho}$ appeared to be negligible as probed by ranging the spin-lock field from 50 to 350 Hz (stronger fields produce undesirable Hartmahn-Hahn[39] and cross relaxation effects).

Temperature of the sample was measured with methanol or ethylene glycol standards.

The saturation-transfer experiments were performed with the saturation field (20−50 Hz) applied at different frequencies (ranging from −0.5 ppm up to 8.5 ppm) of the protein spectrum, which did not overlap with the ligand signals. The spectra were acquired in the direct difference mode: $scan^{saturation\ on\ resonance}$-$scan^{saturation\ off\ resonance}$, with a total of 800 scans per spectrum using CYCLOP phase-cycling.

Docking Protocol. The minimization of the sLe^x/E- and P-selectin complexes were done using the Amber force-field with carbohydrate specific parameters implemented within the Discover program (BIOSYM). The geometry of the ligand was constrained to the conformations found from the transferred-NOE data and docked into the binding site by minimizing ligand/protein distance constraints. The computational protocol consisted of 2000 cycles of conjugate gradient minimization with all selectin residues initially kept fixed. Next, the whole protein/ligand system was subjected to 10 ps constrained molecular dynamics at 300 K followed by another 2000 cycles of conjugate gradient minimization. No water molecules were included in this computation. The P-selectin coordinates were generated on the basis of E-selectin structure and homology modeling.

Computational Details. Computer programs were written in matlab command language (The MathWorks, Inc.) running on SGI Indy R4400 workstation. The nonlinear optimizations were performed using routines contained in the optimization toolbox (The MathWorks, Inc.). Molecular graphics, minimum energy calculations, and processing of the NMR spectra were performed using BIOSYM software.

Conventions. For linkages with GlcNAc as the aglycon, the glycosidic dihedral angles are defined as $\Phi = \tau$(H1-C1-Ox-Cx) and $\Psi = \tau$(C1-Ox-Cx-Hx). For the NeuNAcα2→3Gal linkage, $\Phi = \tau$(C1-C2-O3-C3) and $\Psi = \tau$(C2-O3-C3-H3). The three staggered conformations of the hydroxymethyl group are denoted by gg, gt, and tg, and describe the orientation of the C6−O6 bond relative to the C5−O5 and C5−C4 bonds of the pyranose ring, respectively. The conformation of the glycerol

(29) Sklenár V.; Tschudin, R.; Bax, A. *J. Magn. Reson.* **1987**, *75*, 352−357.
(30) Otting, G.; Wüthrich, K. *J. Magn. Reson.* **1988**, *76*, 569−573.
(31) Titman, J. J.; Neuhaus, D.; Keeler, J. *J. Magn. Reson.* **1989**, *85*, 111−131.
(32) Poppe, L.; van Halbeek, H. *J. Magn. Reson.* **1991**, *93*, 214−217.
(33) Scherf, T.; Anglister, J. *Biophys. J.* **1993**, *64*, 754−76.
(34) Kessler, H.; Oschkinat, H.; Griesinger, C. *J. Magn. Reson.* **1986**, *70*, 106−133.
(35) Kupče, Ē.; Freeman, R. *J. Magn. Reson.* **1992**, *100*, 208−214.
(36) Morris, G. A.; Freeman, R. *J. Magn. Reson.* **1978**, *29*, 433−462.
(37) Bull, T. E. *Prog. NMR Spectrosc.* **1992**, *24*, 377−410.
(38) Davis, D. G.; Perlman, M. E.; London, R. E. *J. Magn. Reson.* **1994**, *104*, 266-275.
(39) Braunschweiler, L.; Ernst, R. R. *J. Magn. Reson.* **1983**, *53*, 521−528.

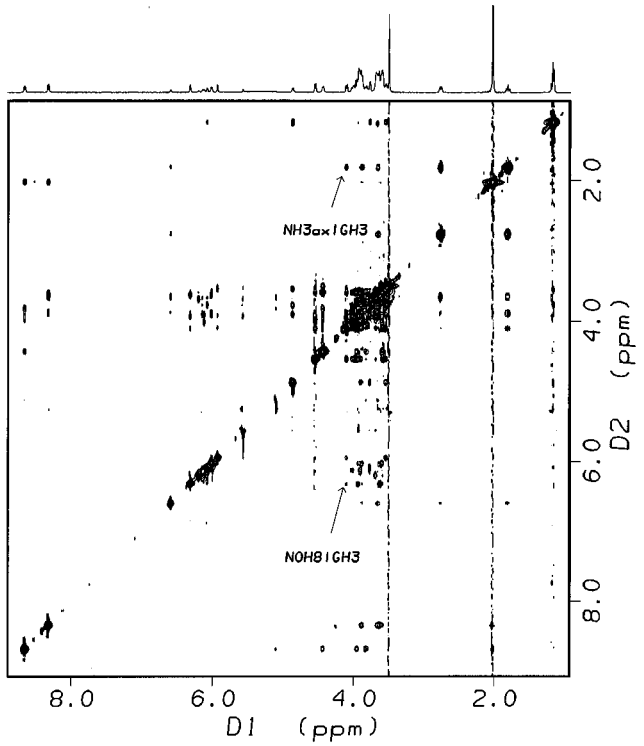

Figure 1. ^{1}H NOESY spectrum (50 ms mixing time, 500 MHz) of **1** in H_2O/D_2O (9:1) at −15 °C. The residual water signal was removed by post-acquisition data processing.

side chain is defined in an analogous way, where, for example, the ggt state denotes the trans arrangement of the first and the second hydroxyl groups. For the hydroxyl groups, three rotamers are defined as anti (180°), g− (60°), and g+ (−60°). The dihedral angles in parentheses are defined by H−O−C−H atoms as positive for a clockwise O−H bond rotation viewing along the C−O bond direction.

Results

Conformation of sLe^x in Water. The conformation of the sLe^x tetrasaccharide (Chart 1) has been investigated by independent groups which arrived at different conclusions regarding rigidity or flexibility of the glycosidic linkages.[4a,b,9] The most recent molecular dynamics and NMR study showed that the branched trisaccharide, F1→3(G1→4)GN, was rigid and the N2→3G linkage was flexible.[9a] Our results reach similar conclusions by a different route. The derivation of the molecular structure in the present study is based entirely on experimental data which include hydroxyl proton NOEs obtained in supercooled water.

The NeuACα2→3Gal linkage conformations were predominantly characterized by the spectral properties of hydroxyl protons. Figure 1 presents the 2D NOESY spectrum of sLe^x in water at −15 °C. The indicated NOH8/GH3 and NH3ax/GH3 contacts cannot occur in a single conformation as shown on the distance map[40] in Figure 2. Thus, this linkage must occur in more than one conformation in solution. During this calculation the sialic acid side-chain was fixed in the ggt state as inferred from the strong NOH8-NH6 and NOH8-NH8 NOE effects (Figure 1). Also the slow chemical exchange rate and small vicinal coupling constant for the NOH8 proton (Table 1) strongly indicate the existence of NCOOH:::NOH8 hydrogen bonding.[41]

(40) Poppe, L.; von der Lieth, C. W.; Dabrowski, J. *J. Am. Chem. Soc.* **1990**, *112*, 7762−7771.

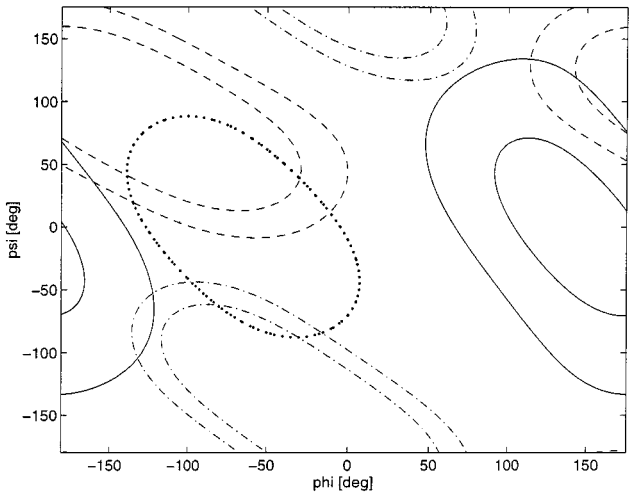

Figure 2. Distance map demonstrating the flexibility of the NeuAcα2→3Gal linkage. The fields enclosed between the solid lines and dotted lines correspond to NH3ax/GH3 (2−3 Å) and NOH8/GH3 (<4 Å) distance constraints, respectively. The filelds enclosed between the dashed lines and dash-dotted lines correspond to GOH2:::NO6 and NCOO:::GO4 hydrogen bond constraints (2.6−3.2 Å), respectively.

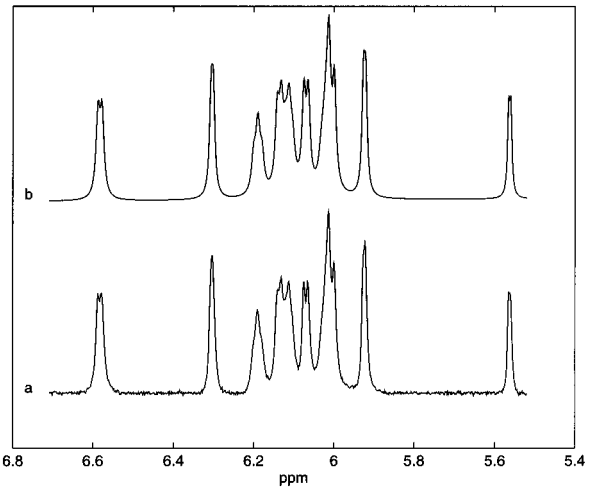

Figure 3. Experimental (a) and theoretical (b) hydroxyl proton portion of ^{1}H spectrum of **1** in H_2O/D_2O (9:1) solution at −15 °C. The parameters obtained from the total lineshape analysis (b) are listed in Table 1.

Hydroxyl proton resonances at supercooled conditions of water are shown in Figure 3a. All signals were fitted by the total line shape analysis[42] (Figure 3b) which yielded vicinal coupling constants and chemical exchange rates with the solvent protons (Table 1). There is a remarkable difference between spectral parameters for the GOH2 proton in sLe^x and the Le^x trisaccharide. We observe a large upfield shift of 0.7 ppm in the case of tetrasaccharide (see Supporting Information) together with the reduction of the vicinal coupling constant and chemical exchange rate. These spectral changes closely follow the behavior of the glucose-OH3 proton in methyl-β-lactoside[10] and strongly indicate the formation of the intramolecular hydrogen bonding GOH2:::NO6 in the sLe^x tetrasaccharide (compare Figure 2).

Transformation from the Le^x into the sLe^x produces spectral changes for the GOH4 proton as well. In this case the chemical shift effect is negligible, although there is a significant reduction of the vicinal coupling constant (∼2 Hz) and chemical exchange

(41) Poppe, L.; van Halbeek, H. *J. Am. Chem. Soc.* **1991**, *113*, 363−365.

(42) Rao, B. D. N. *Methods Enzymol.* **1989**, *176*, 279−311.

Table 1. NMR Data for Hydroxyl Protons from sLe^x in H_2O/D_2O (9:1) at −15 °C

hydroxyl proton	shift[a] [ppm]	coupling ^3J[b] [Hz]	rate[c] [s^{-1}]
GN-OH6	6.1	4.5; 4.9	10.1
F-OH2	n.d.	n.d.	n.d.
F-OH3	6.11	5.0	7.3
F-OH4	6.07	5.5	5.9
G-OH2	5.93	2.9	1.8
G-OH4	5.56	2.7	∼0
G-OH6	6.19	4.8; 5.8	7.9
N-OH4	6.58	5.0	6.7
N-OH7	6.00	7.1	5.0
N-OH8	6.31	2.8	2.7
N-OH9	6.01	4.3; 5.7	12.4

[a] Chemical shifts relative to the water resonance at 5.28 ppm. [b] Estimated errors were ±0.3 Hz for the primary and ±1 Hz for the secondary hydroxyl protons. [c] Estimated errors were ±2 s^{-1}.

Table 2. NMR Constraints Used for Modeling the Le^x Part of sLe^x

constraint	value range[a]	rotameric states[b]
GH1-GNH4	2.5 ± 0.3 Å	
GH1-GNH6R	2.5 ± 0.5 Å	gg
GOH2-GNH6R	2.5 ± 0.5 Å	g+, gg
FH1-GNH3	2.5 ± 0.3 Å	
FH5-GH2	2.5 ± 0.3 Å	
FH3-GH6S	2.8 ± 0.5 Å	gt
FH4-GOH4	3.0 ± 0.5 Å	g−
$FCH3^{CM}$-GH2	2.8 ± 0.5 Å	
FH4-GH6S	2.8 ± 1.0 Å	gt
$^3J_{GH1-GNC4}$	3.0 ± 1.0 Hz	
$^3J_{GC1-GNH4}$	5.3 ± 1.0 Hz	
$^3J_{FH1-GNC3}$	2.5 ± 1.0 Hz	
$^3J_{FC1-GNH3}$	4.8 ± 1.0 Hz	

[a] The distance constraints were obtained from the 2D NOESY and and 1D DAISY-NOESY experiments at 285 K in D_2O or at 268 K in H_2O/D_2O (9:1). Internuclear distances were calculated from the formula $r_{ij} = (\sigma_o/\sigma_{ij})^{1/6}/r_o$, where σ_o and r_o are the cross-relaxation rate and distance for the reference proton pair, respectively. The uncertainties for the internuclear distances are conservative, *i.e.*, they exceed distance variations due to the different choices of r_o and experimental errors for σ_{ij} and σ_o. In the case of pendant groups they were estimated as described previously.[43] The precision of the coupling constants is equal to the digital resolution in the spectra (0.35 Hz/pt). The larger error margins account for the inaccuracy of eq 3. [b] During optimization of the ligand geometry pendant groups were frozen in the single rotameric state.

rate. As inferred from the molecular model, these observations are consistent with the NCOOH:::GOH4 hydrogen bond (compare Figure 2).

In the case of the Fuc1α→3[Galβ1→4]GlcNAc portion the NOE data show no evidence for multiple conformations. Table 2 shows NOE derived distances and vicinal coupling constants used in the calculation based on eq 1. Allowable solutions fell into the narrow range of dihedral angles: {45.6° ± 1.2°; 17.7° ± 1.7°} for the Galβ1→4GLcNAc linkage and {47.9° ± 1.8°, 23.7° ± 1.0°} for the Fucα1→4GlcNAc linkage. The possibility that Fucα1→3GlNAc linkage samples {−23°, −15°} conformation, as was recently suggested,[44] may be safely ruled out on the basis of NOE data in Table 2.

Conformation of the sLe^x Bound to E-Selectin. Dissociation rate, k_{off}, and equilibrium binding constant, K_D, for this complex (Table 3) were obtained from the nonlinear fitting of the NH3eq relaxation data as described in Methods. These data were used in the quantitative analysis of transferred-NOE spectra.

(43) Poppe, L.; Dabrowski, J.; Lieth, C. W.; Koike, K.; Ogawa, T. *Eur. J. Biochem.* **1990**, *189*, 313−325.

(44) Lommerse, J. P. M.; Kroon-Batenburg, L. M. J.; Kroon, J.; Kamerling, J. P.; Vliegenthart, J. V. G. *J. Biomol. NMR* **1995**, *5*, 79−94.

Table 3. Equilibrium Binding Constant and Dissociation Rates for the Binding of sLe^x to E-, P-, and L-Selectins

	sLe^x/E-selectin[a]	sLe^x/P-selectin[a]	sLe^x/L-selectin[b]
K_D (at 300 K)	0.72 ± 0.12 mM	7.8 ± 1.0 mM	3.9 ± 0.7 mM
k_{off} (at 300 K)	164 ± 24 s^{-1}	522 ± 166 s^{-1}	1080 ± 167 s^{-1}

[a] Obtained from the fitting of the relaxation rates. [b] Obtained from the simultanous fitting of 256 signal intensities. Error limits were calculated by using Monte Carlo sampling technique.[49]

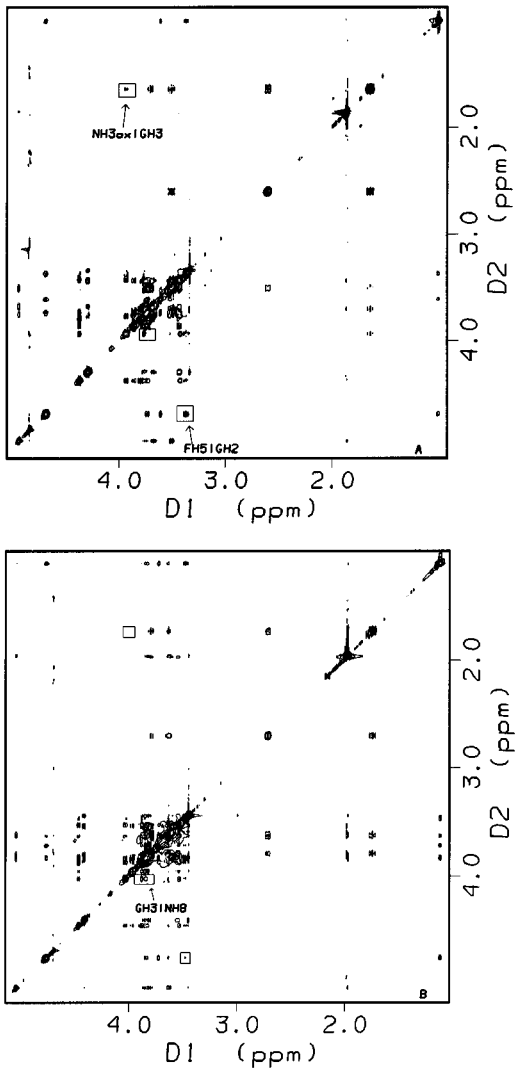

Figure 4. (a) ^1H NOESY of sLe^x in D_2O at 285 K (500 ms mixing time, 500 MHz). (b) Tranferred NOESY of sLe^x/E-selectin (21:1) in D_2O at 300 K (500 ms mixing time, 500 MHz). The most apparent differences between both spectra are indicated with the boxes.

Most apparent differences between the NOE fingerprints for the free and E-selectin bound ligand are noted in Figure 4. The disappearance of the NH3ax/GH3 and significant enhancement of GH3/NH8 cross-peaks indicate that the conformation of the NeuAcα2→3Gal linkage has changed upon binding. Another striking observation is the significant diminution of the GH2-FH5 NOE interaction. However, any further interpretation of the data in terms of relative changes in ligand conformation is far from straightforward. The relatively slow off-rate and strong motional anisotropy of the protein (see Methods) necessitate more rigorous treatment. The bound state conformation of sLe^x was derived from full relaxation matrix analysis of the transferred-NOE data taking into account motional anisotropy of the complex.

It is important to mention that the computational protocol (see Methods) did not include protein protons in the treatment

Table 4. Conformations and Orientations of sLe^x complexed to E-, P-, and L-Selectins[g]

calculation[a]	conformation[b]	orientation[c]	R[d]
sLe^x [e]	{46 ± 1, 18 ± 2; 48 ± 2, 24 ± 1}		
sLe^x/E-selectin			
	{−60,-17;20,36;72,13}	{120, 86};{75, 30}	0.14
	{−53,-27;29,32;69,15}	{114,80};{70, 25}	0.15
average[f]	{−58 ± 5,-22 ± 5;24 ± 5;34 ± 3;71 ± 3,14 ± 2}		
sLe^x/P-selectin			
P1	{−74,-8;45,21;68,21}	{57, 30};{20, 60}	0.12
	{−91,6;46,18;68,22}	{52; 46};{30, 70}	0.13
	{−76,4;52,21;48,33}	{57,30};{20, 60}	0.14
P2	{−102,11;43,11;53,24}	{143, 29};{95, 10}	0.14
average	{−85 ± 11,-4 ± 12;45 ± 4,18 ± 4;61 ± 10;26 ± 6}		
sLe^x/L-selectin[e]	{36,28;41;16}		
	{45,20;28,17}		
	{25,29;47,14}		
average	{33 ± 10,26 ± 12;42 ± 11,16 ± 3}		

[a] Different minima reached during the optimization of the target function, T (eq 4). [b] Pairs of dihedral angles in curly braces correspond to NeuAcα2→Gal, Galβ1→4GlcNAc, and Fucα1→4GlcNac linkages, respectively. [c] The values in the first curly braces correspond to the polar angles, θ and ϕ, describing the orientation of the major diffusional axis in the molecular frame of the ligand. The values in the second curly braces correspond to the angles between major axis of rotational diffusion tensor and vectors formed by the GNH4-NH3ax and NC9-FC6 atom pairs, respectively. [d] R factors were calculated according to the following formula:

$$R = \left\{ \frac{\sum_{ijm}^{N} [I_{ij}^{\exp}(\tau_m) - I_{ij}^{\mathrm{calc}}(\tau_m)]^2}{\sum_{ijm}^{N} [I_{ij}^{\exp}(\tau_m)]^2} \right\}^{1/2}$$

[e] Only the conformation of Le^x part was calculated from NMR data (eq 1). [f] The average values and standard deviations were calculated from the results of minimizations corresponding to the different sets of starting conditions (see Text). [g] All values were rounded to the nearest integer.

of relaxation. In order to justify this simplification we performed the transferred-2D NOESY experiment, where during the mixing time (500 ms) protein magnetization was saturated at two different frequencies, within aromatic and aliphatic regions, by the DANTE pulse train. Due to the effective spin-diffusion within protein protons, indirect transfers, $H_{L1} \rightarrow H_P \rightarrow H_{L2}$, if operative, should be eliminated or at least strongly attenuated.[37] However, the resulting spectrum was almost identical to the nonsaturated version (not shown). Thus the exclusion of protein protons in the analysis is justified.

The conformations are listed in Table 4 where the different sets of dihedral angles were chosen to demonstrate maximum differences which resulted from the optimizations. It appears that the bound conformation of sLe^x to E-selectin is uniquely defined. The NeuAcα2→3Galβ1 is locked at {−60°, 0°}, probably stabilized by the intraligand NCOOH:::GOH2 hydrogen bonding.

SLe^x-O-Ac Derivative. At this point it is instructive to compare some of the results obtained for the sLe^x derivative in which the GOH2 group was replaced by −OAc. The methyl protons from this group appeared to be an excellent conformational probe for the free as well as for the bound ligand. For this derivative the NeuAcα2→3Gal linkage is also disordered in the free state and stays close to the {−60°, 0°} conformation when sLe^x-OAc is bound to E-selectin (see Supporting Information). Here, the absence of transferred-NOE for the GH3/NH3ax and G-O-CH3/NH3eq protons, the very weak effect for the G-O-CH_3/NH3ax protons, and the presence of the G-O-CH_3/NH8, G-O-CH_3/NH5 and GH3/NH8 interactions can only occur when $\{\Phi_I, \Psi_I\}$ sample values near {−60°, 0°}. As expected, sLe^x-OAc showed the same binding affinity to E-selectin as sLe^x (unpublished data).

Conformation of the sLe^x Bound to P-Selectin. The measurement of the off-rate and equilibrium binding constant showed very weak binding in this case (Table 3). The bound conformation was calculated from the full relaxation-matrix analysis of the 2D transferred-NOE spectra as described in Methods. The data are consistent with two solutions, P1 and P2 in Table 4, which have quite different orientations. The NeuAcα2→3Gal linkage adopts a conformation similar to E-selectin, which is consistant with the formation of the NCOOH:::GOH2 hydrogen bonding (see Figure 2)

Conformation of sLe^x Bound to L-Selectin. The conformation of sLe^x was derived in this case from the first-order analysis of the 2D transferred-NOESY spectrum. The interproton distances (Table 5) were calculated by using an isolated two-spin approximation.[12a] This approximation is reasonable in this case since the Y shaped, sLe^x/L-selectin-Ig complex probably tumbles in solution more isotropically than the E- and P-selectin complexes. In addition, the cross-peak intensities are not biased by the slow k_{off} rate (Table 3).

Allowed conformational space for the NeuAcα2→3Galβ1 linkage is obtained from the distance map shown in Figure 5. This map was constructed from two interresidue GH3-NH8 and GH3-H3ax constraints and one negative GH2-N3ax constraint, for which no NOE effect was observed.[9c] The allowed conformational space (black) encloses the {−100°, −50°} conformation, which was independently postulated from the minimum energy calculations.[45] Since this conformation is predominantly determined by the presence of GH3-H3ax NOE (see Supporting Information) it is important to note that this NOE is completely absent in transferred-NOE spectra for E-selectin and is barely distinguishable from the noise in the spectra for P-selectin. Interestingly the $\{\Phi_I, \Psi_I\}$ values close to {−100°, −50°} allow for the formation of the GOH4::: NCOOH hydrogen bonding which was also deduced from the hydroxyl-proton data for the free ligand (vide supra). The conformation of the Fuc1α→3[Galβ1→4]GlcNAc fragment was modeled from the NOE data in Table 5 and by minimizing the objective function defined in eq 1 without J couplings. The

(45) Berg, J; Kroon-Batenburg, L. M. J.; Strecker, G.; Montreuil, J.; Vliegenthart, J. F. G. *Eur. J. Biochem.* **1989**, *178*, 727−739.

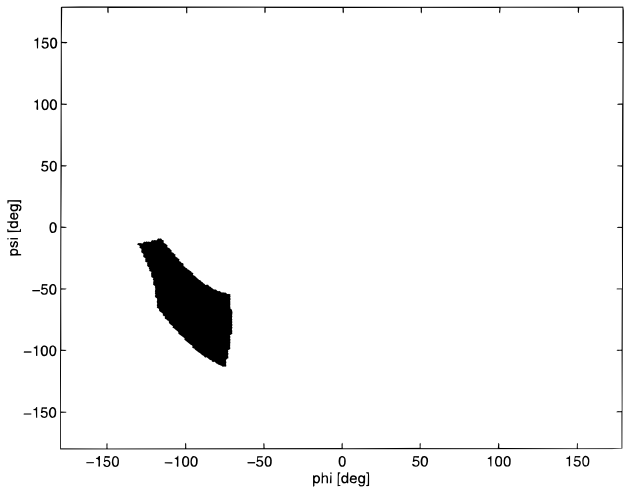

Figure 5. NOE distance map for the NeuAcα2→3Gal linkage conformation in the sLe^x/L-selectin complex. The marked area designates the overlap GH3/NH3ax, NH8/GH3, and GH2/NH3ax constraints, where the last constraint is negative (>4 Å).

Table 5. Distance Constraints Obtained from Tranferred NOE Experiment for sLe^x Bound to L-Selectin

contact	distance range[a] [Å]
NH3ax-GH3	3.5 ± 0.5
NH8-GH3	3 ± 0.5
GH1-GNH4	2.5 ± 0.3
GH1-GNH6R	2.5 ± 0.5
FH1-GNH3	2.5 ± 0.3
FH5-GH2	3 ± 0.3
FH1-GNNCO$\underline{CH_3}^{CM}$	3.5 ± 0.5
FCH_3^{CM}-GH2	3.2 ± 0.4

[a] The error bounds were obtained in the same way as described in Table 2.

results of these calculations are summarized in Table 4. Fewer distance constraints in this case produce larger uncertainties in glycosidic angles. However, no significant departures from the conformation of the free ligand are apparent in the L-selectin bound state.

E- and P-Selectin-Ig Fusion Proteins. Possible variations in the arrangement of the trisaccharide part are not so obvious in the presence of the observational uncertainties. Substantial attenuation of the GH2-FH5 interaction upon binding to all selectins could result either from conformational change or motional anisotropy. Interestingly, the GH2-FH5 distance was calculated to be significantly shorter for the P- as compared to the E- and L-selectin complexes (∼2.5 Å *vs* ∼3 Å). Thus if motional anisotropy is decreased one should observe significantly different strengths of FH5-GH2 NOE for P- as compared to E-selectin. This was verified by recording transferred-NOE spectra for the E-selectin-Ig and P-selectin-Ig constructs. These molecules have the same CRD domains as the recombinant E- and P-selectin, but their overall shapes are completely different. It is reasonable to assume that these fusion proteins tumble more isotropicaly than the recombinant proteins. This is especially true for P-selectin-Ig, which has only two of the nine complement regulatory modules present in recombinant P-selectin. Indeed, in all recorded spectra, the GH2-FH5 NOE consistently appeared as a relatively strong interaction only in the sLe^x/P-selectin-Ig complex (see Supporting Information). However, the differences in signal intensities correspond to the interproton distance variations of ca. 0.3−0.4 Å which may be readily achieved by a minor adjustment of dihedral angles.

Ligand-Protein Contacts. Our study shows that the galactose residue in sLe^x makes close contacts with all three selectins.

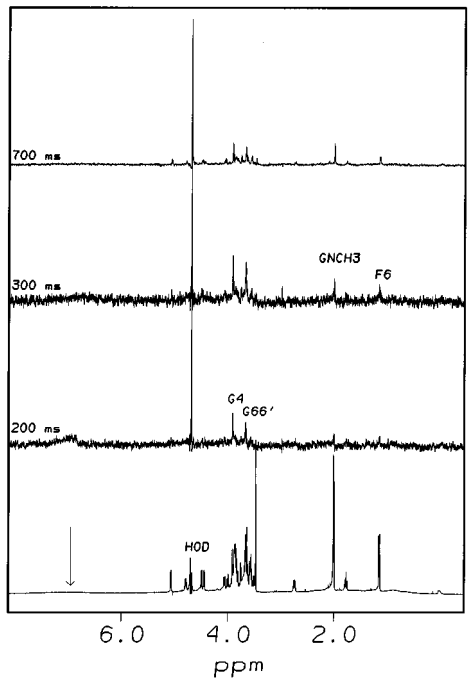

Figure 6. The bottom trace corresponds to ^{1}H spectrum of sLe^x/E-selectin (40:1). The upper traces correspond to the magnetization transfer experiments with the different length of presaturation time. The marked proton signals originate from the protein to ligand magnetization transfer effect. The arrow points at the frequency of the saturating field.

Saturation-transfer experiments showed that for both E- and P-selectin the GH4 and GH66′ protons are making close contacts while only GH4 makes close contact with the L-selectin (see Supporting Information). The largest saturation transfer effect was achieved when the frequency of the saturating field being within the aromatic region in all protein spectra. From the examination of 3D models it follows that unless there is some major conformational change in the protein, Tyr 48 and Tyr 94 are the only candidates to make these contacts with the galactose. When the irradition times get longer the entire ligand is heated up, as shown for the E-selectin complex in Figure 6. The same effect was observed for the P-selectin at lower temperatures and very weak secondary magnetization transfers were observed for L-selectin, consistent with the measured differences of k_{off} values (see Table 3). Computational docking experiments (Figure 7) confirmed that sLe^x can be aligned with both E- and P-selectin such that Fuc-OH2 and Fuc-OH3 hydroxyls complex the selectin calcium atom,[46,47] while galactose H4, H66′ protons are situated within 5 Å distance of the aromatic protons of Tyr 48 and Tyr 94. In this alignment the carboxylic group from sialic acid might be involved in hydrogen bonding with Tyr 48, which is present in both selectins. Assuming similar orientations of the ligand within E- and P-selectin (P2 solution in Table 4) one may speculate that the early transfer of magnetization to the GlcNAc -O-CH_3 (3.3 ppm) and -N-CO-CH_3 (2 ppm) protons, which occurs only in the case of P-selectin, is caused by the proximity of these protons to His 108, replacing arginine in E-selectin. This model is consistant with amino acids shown by mutagenesis studies to be essential for sLe^x binding to both E and P selectin[3,5,6] and with the chemical modifications to sugar hydroxyl protons which showed that Gal-OH4 and Gal-OH6 must be involved in the recognition.[7b,f,h]

(46) Weis, W. I.; Kahn, R.; Fourme, R.; Drickamer, K.; Hendrickson, W. A. *Science* **1991**, *254*, 1608−1615.
(47) Ng, K. K. S.; Drickamer, K.; Weis, W. I. *J. Biol. Chem.* **1996**, *271*, 2, 663−674.

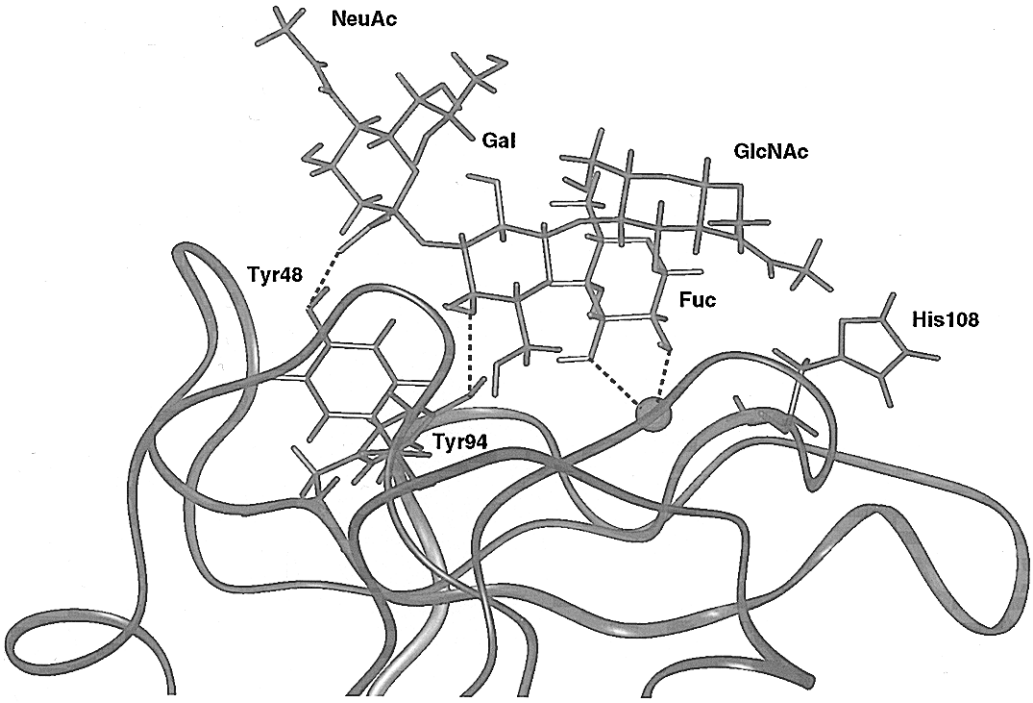

Figure 7. Possible alignment of sLe^x with P-selectin (only the part of the CRD domain is shown). The interactions discussed in the text are marked with the dotted lines.

Discussion

During the conformational analysis, carbohydrate side-chains were frozen in predefined rotameric states, a simplification justified by the following experimental observations. In the case of sialic acid, the glycerol side-chain is characterized by very small NH6−NH7 (∼1 Hz) and fairly large NH7−NH8 (∼8 Hz) vicinal coupling constants, corresponding to *gauche* and *trans* proton arrangements, respectively, and by the strong hydrogen bond: NOH8:::COOH.[41] Also ^{13}C relaxation data for the GD1a ganglioside in the micellar state[48a] showed that sialic acid side chain remains rigid up to the C8 carbon. Unfortunately, corresponding data are not available for the bound state. Nevertheless, the side-chain conformation can be deduced from certain NOE patterns. Fortuitous nonoverlap of spectral lines allowed observation of such a pattern for the E-selectin/sLe^x-OAc complex. Here, strong NH6−NH7 and weak NH6−NH8 and NH7−NH8 interactions indicate conformational similarity between the free and bound state (see Supporting Information). Moreover, fairly strong NH8/GH3 contacts, observed for all complexes, allow for unambiguous sign assignment of H6−C6−C7−H7 and H7−C7−C8−H8 dihedral angles. For the hydroxymethyl group of the galactose residue, the observed contacts between GH66′ and FH6, FH4 or FH3 are consistent with either gt or tg conformation. Finally, the hydroxymethyl group of the glucose residue most likely occupies the gg state when bound to selectins. This is shown by stronger GH1-GNH6^R compared to GH1-GNH6^S cross-peak intensity, especially for short mixing times in transferred-NOESY spectra. For the gt rotamer this pattern would be reversed and for the tg state both interactions would vanish.

Conformational flexibility of NeuAcα2→3Gal has been previously demonstrated in other carbohydrate molecules.[48] In the absence of steric hindrance the conformations with {Φ, Ψ} values close to {180°, 0°}, {−60°, 0°}, and {−100°, −50°} are possible according to the minimum energy calculations.[45] We have shown that {−60°, 0°} and {−100°, −50°} conformations are partially stabilized by the intramolecular hydrogen bonds: NO6:::GO2 and NCOO:::GO4, respectively. Interestingly, the {−60°, 0°} conformation seems to be populated in the free ligand even after removal of the NCOOH:::GOH2 interaction, as shown by the Gal-OAc derivative of sLe^x . The time scale of the conformational transitions for this linkage was estimated to be in the subnanosecond range as obtained from ^{13}C[48a] and ^{1}H[48b] relaxation measurements. In other sugars, the same linkage may be sterically restricted to the {180°, 0°} conformation by the adjacent galactose residue as it occurs in Galβ(1→4)[NeuAcα(2→3)]Gal molecular fragment.[48a,d] Since the NH3ax-GH3 NOE is *ca*. ten times weaker in the sLe^x than in the GM1[48d] or GD1a[48a] gangliosides, the {180°, 0°} conformation should be minor in the selectin ligand. The presence of the {−100°, −50°} conformation in the free sLe^x was inferred from the spectral behavior of the GOH4 hydroxyl proton. However, relatively large 4.7 ± 0.4 Hz, $^3J_{NC2-GH3}$ coupling constant shows that the Ψ_I dihedral spends most of the time in the vicinity of 0° and indicates that the population of the {−100°, −50°} conformer is low as well. Thus the major conformation in sLe^x is {−60°, 0°}.

Flexibility of the NeuAcα2→3Gal linkage seems to be related to the specificity of sLe^x epitope for different selectins. Our analysis of the bound ligand revealed that both E- and P-selectin recognize the {−60°, 0°} conformer, while the {−100°, −50°} conformation is probably recognized by L-selectin.

Alignment of sLe^x with E- and P-selectin has been proposed by several groups,[1b,2b,3,5] inspired by the X-ray structure of CRD-EGF domain of E-selectin[3] and X-ray structure of mannose binding protein.[46] It is widely believed that fucose, in analogy to mannose in MBP, chelates the calcium atom through OH2 and OH3 hydroxyls,[47] also shown in Figure 7. One should note, however, that this alignment is not the same as the calculated orientations (Table 4) which are referred to the major axis of the moment of inertia tensor obtained from X-ray

(48) (a) Poppe, L.; van Halbeek, H.; Acquotti, D.; Sonnino, S. *Biophys. J.* **1994**, *66*, 1642−1652. (b) van Halbeek, H.; Poppe, L. *Magn. Reson. Chem.* **1992**, *30*, S74−S86. (c) Poppe, L.; Dabrowski, J.; von der Lieth, C. W.; Numata, M.; Ogawa, T. Eur. *J. Biochem.* **1989**, *180*, 337−342. (d) Acquotti, D.; Poppe, L.; Dabrowski, J.; von der Lieth, C. W.; Sonnino, S.; Tettamanti, G. *J. Am. Chem. Soc.* **1990**, *112*, 7772−7778.

coordinates of E-selectin CRD-EGF domain. For example, the angles between (NH3ax-GNH4, FC6-NC9) vectors and the major axis are (70°, 30°) from the fitting of transferred-NOE spectra compared to (95°, 83°) obtained from the docking protocol. One likely explanation for this discrepancy would be that the CRD is not oriented along the major axis of the ellipsoid. Further work would be necessary to elucidate this situation.

SLe^x binds weakly to all three selectins, although the natural ligands for selectins probably extend beyond the tetrasaccharide structure.[50,51] The differences in the equilibrium binding constants obtained for the three selectins are in good agreement with inhibition assays (unpublished results) and with published data.[7de,52] Interestingly, the large difference between off-rates for E- and L-selectin (Table 3) is in agreement with the recent study,[51] which showed that unlike E-selectin, L-selectin does not support cell rolling.

Conclusions

This paper presents new approaches to the conformational analysis of the sLe^x tetrasaccharide, free in solution and bound to E-, P-, and L-selectin receptors. The NMR-derived parameters, which included hydroxyl proton resonances in water, were used to construct three-dimensional structures of the free and bound ligand. In the free state, the NeuAcα2→3Gal linkage samples conformations in the vicinity of {180°, 0°}, {−60°, 0°}, and {−100°, −50°}. The latter two conformers are partially stabilized by the GOH2:::COOH and GOH4:::COOH hydrogen bonds, respectively. The transferred-NOE analysis revealed that E- and P-selectin bind to the {−60°, 0°} conformer, although the Φ_I in the P-selectin complex might reach values up to −100°. On the other hand, the {−100°, −50°} orientation is preferred when sLe^x is bound to L-selectin. The conformations of the trisaccharide fragment are similar in all situations where the maximum difference (∼30°) was obtained for the Φ_{II} dihedral angle.

The dissociation rates and equilibrium binding constants were readily obtained from the selective proton relaxation studies. This avoided the assumption of diffusionally controlled association process, a common practice for estimation of k_{off} rates in transferred-NOE studies. In fact, the kinetic on-rates for selectin binding, $\sim 10^5\ s^{-1}\ mol^{-1}$, appeared to be much slower then the diffusional limit.

Strong anisotropy of molecular tumbling complicates data analysis but allows one to obtain significantly more information about 3D structures as compared to the case where the receptor has globular or irregular shape (L-selectin-Ig) and reorients in solution more chaotically. With the well defined anisotropic model of motion, all NOE interactions, both inter- and intraresidue, contribute to the determination of the bound conformation of the ligand and to the determination of the ligand orientation relative to the major axis of the rotational diffusion tensor. This approach which allowed us to better define the bound conformations of sLe^x to E- and P-selectin could be even more fruitful if applied to other protein bound carbohydate ligands which usually display a small number of interresidual distance constraints.

Although the model for the carbohydrate−selectin complex still remains imprecise, the information obtained in this study confirms that the galactose residue from the sLe^x ligand has an important role in molecular recognition, and its presence should not be ignored in the design of new selectin inhibitors.[53]

Acknowledgment. Thanks to André Venot for many stimulating discussions, Richard Nelson for E-, P-, and L-selectin-Ig constructs, Kevin Moore for recombinant P-selectin, Richard Cummings for running biological assays, and Guy Vigers for careful reading of the manuscript.

Supporting Information Available: List of experimental cross-peak intensities from the transferred-NOE spectra for the sLe^x/E-selectin and sLe^x/P-selectin complexes, relaxation rates for H3eq proton in different complexes, thermodynamic and kinetic parameters for binding of sLe^x to all three selectins, 2D COSY for Le^x trisaccharide in water, transferred-NOESY for sLe^x/P-selectin, sLe^x-OAc/E-selectin, and sLe^x/L-selectin sLe^x/E,P-sel-Ig complexes, 2D NOESY data for the sLe^x-OAc derivative, the distance map for the NeuAcα2→3Galβ linkage, and the saturation transfer experiments for P- and L-selectin complexes (18 pages). See any current masthead page for ordering and Internet access instructions.

JA9610702

(49) Alper, J. S.; Gelb, R. I. *J. Phys. Chem.* **1990**, *94*, 4747−4751.
(50) Sako, D.; Comess, K. M.; Barone, K. M.; Camphausen, R. T.; Cumming, D. A.; Shaw, G. D. *Cell* **1995**, *83*, 323−331.
(51) Kolbinger, F.; Patton, J. T.; Geisenhoff, G.; Aenis, A.; Li, X.; Katopodis, A. G. *Biochemistry* **1996**, *35*, 6385−6392.
(52) Brandley, B. K.; Kiso, M.; Abbas, S.; Nikrad, P.; Srivasatava, O.; Foxall, C.; Oda, Y.; Hasegava, A. *Glycobiology* **1993**, *3*, 633−639.
(53) Wu, S.-H.; Shimazaki, M.; Lin, Ch.-Ch.; Moree, W. J.; Weitz-Schmidt, G.; Wong, C.-H. *Angew. Chem., Int. Ed. Engl.* **1996**, *35*, 88−90.